Composite Structures 223 (2019) 110964

Contents lists available at ScienceDirect

Composite Structures

journal homepage: www.elsevier.com/locate/compstruct

Influence of mechanical uncertainties on dynamic responses of a full-scale all-FRP footbridge

Xiaojun Wei[a,c], Hua-Ping Wan[b,*], Justin Russell[c], Stana Živanović[d], Xuhui He[a]

[a] School of Civil Engineering, Central South University, Changsha 410075, China
[b] College of Civil Engineering and Architecture, Zhejiang University, Hangzhou 310058, China
[c] School of Engineering, Warwick University, Coventry CV4 7AL, United Kingdom
[d] College of Engineering, Mathematics and Physical Sciences, University of Exeter, Exeter EX4 4QF, United Kingdom

ARTICLE INFO

Keywords:
Uncertainty quantification
Global sensitivity analysis
Statistical characteristics
Polynomial chaos expansion
All-FRP footbridge
Dynamic response

ABSTRACT

This paper aims to determine the effects of uncertainties in the mechanical properties of FRP composites on the dynamic responses of a full-scale all-FRP bridge. The novelty of the study is in determining the effects that the uncertainties have on the global structural scale properties rather than component properties often studied in literature. To achieve this aim, both uncertainty quantification and global sensitivity analysis are performed using a computationally cost-effective approach based on the polynomial chaos expansion. The results reveal that a coefficient of variation (COV) of 10% for four mechanical parameters can lead to COVs of 3.37%, 2.92% and 3.07% for natural frequencies, COVs of 2.98%, 0.04% and 0.61% for modal masses (corresponding to unity-scaled mode shapes) of the first lateral, first vertical and second vertical modes, and COV of 0.93% for the absolute peak acceleration. The effect of uncertainties, therefore, is very small for the considered excitation case and it could be neglected in the design. In addition, it was found that the longitudinal elastic modulus and shear modulus of the panel are the most influential mechanical parameters in dynamic analysis.

1. Introduction

Glass fibre reinforced polymers (FRPs) have increasingly been utilised for the construction of bridges due to their high strength- and stiffness-to-weight ratios, low maintenance costs and quick installation. Due to their lightweight nature, FRP bridges may be very lively and potentially suffer excessive vibration [1,2] causing user discomfort. Therefore, vibration serviceability is increasingly governing the design of FRP bridges [3]. A wider use of FRP materials for structural applications is being prevented by the lack of nationally or internationally recognised design standards [3,4]. The underdeveloped guidance for vibration serviceability design is attributed to the limited information on the dynamic properties of FRP structures and vibration performance under dynamic actions, e.g. pedestrian and wind excitations.

Currently, the influence that uncertainties in mechanical properties have on the dynamic performance of FRP structures is unknown and cost-effective approaches for quantifying this influence are required. Manufacturing FRP composites involves complex processes characterised by uncertainties, such as variations in fibre orientations and fibre volume fractions, matrix material uncertainties, and variations in environmental parameters and process conditions. The complexity of the manufacturing process makes the quality of FRP products difficult to control, which might lead to considerable differences between the actual mechanical properties and those specified in the design process [5]. As a consequence, the dynamic properties of FRP structures and the resulting vibration response might be difficult to predict accurately. Although a probability-based load and resistance factor design philosophy that accounts for uncertain mechanical properties has been employed for the static design for FRP structures [6], there is no such counterpart for vibration serviceability. Conventional design criteria for dynamic design, by simply limiting the fundamental frequency or static deflection, may underestimate or overestimate the dynamic performance of FPR structures and result in either over-conservative, cost-ineffective designs or unserviceable structures. Therefore, developing the knowledge about the effects of uncertainties in mechanical properties on the dynamic responses and providing a computational means for time-effective quantification of these effects are crucial requirements for formulating guidelines and standards for the vibration serviceability design of civil engineering FRP structures.

Most of the existing research is devoted to uncertainty quantification (UQ) in the dynamic analysis of FRP composite components, e.g. plates, beams or shells. Piovan et al. [7] studied the stochastic dynamics

* Corresponding author.
E-mail address: huaping.wan@gmail.com (H.-P. Wan).

https://doi.org/10.1016/j.compstruct.2019.110964
Received 26 November 2018; Received in revised form 6 May 2019; Accepted 7 May 2019
Available online 10 May 2019

of composite I-beams and box beams with variations in fibre orientation angles in the laminate and elastic properties of a ply (i.e. longitudinal and transverse elastic modulus, shear modulus and Poison ratio). They employed the Monte Carlo simulation (MCS) method to obtain the statistics of dynamic properties (i.e. natural frequencies and frequency response functions) and showed that the sensitivity of the dynamic responses to uncertainty sources depends upon stacking sequence. Dey et al. [8] performed the UQ of natural frequencies, frequency response functions and mode shapes of a laminated cantilever plate with fuzzy variation in ply orientation and in material properties at the ply scale. They used polynomial chaos expansions (PCE)-based method and found it to be computationally efficient compared with the global optimisation approach for uncertainty propagation of fuzzy variables. Sepahvand [9] focused on the quantification of the effects of the random fibre orientation in a 12 plies laminate plate on its natural frequencies and mode shapes using the PCE-based method. He found that the COV of 10% for the fibre orientation gave rise to the COVs of no more than 6% for the natural frequencies of the first fifteen modes. Additionally, the uncertainty in the fibre orientation caused different mode shapes for the 10th and 11th modes compared with their nominal counterparts. Awrush and Gomes [10] considered the control problem in a laminated composite plate embedded with piezoelectric patches. A fuzzy interval analysis methodology was employed to investigate the impact of uncertainties in the material properties of the composite plate and piezoelectric patches on natural frequency, mechanical vibration and electric control input energy. Allegri et al. [11] investigated a virtual planar composite truss for space applications (6 m long and 1 m wide), which has 25 members of identical circular cross-section, using an approach based on the Monte Carlo evaluation of finite element stochastic weighted integrals. Their analysis showed that the COVs of 15% for Young's and shear modulus and the COV of 5% for mass density can lead to the COVs of 16.1% and 14.7% for the natural frequencies of 2nd and 3rd modes, respectively.

Unlike UQ, there is limited insight into the sensitivity of dynamic responses of FRP components to material parameters. Carvalho et al. [12] utilised a multivariable linear regression analysis to assess the sensitivity of the fundamental frequency of a laminated composite plate to the thickness of each ply, several mechanical properties of the material, and fibre orientation angles. They found that the fundamental frequency is most sensitive to laminate thickness, followed by longitudinal elastic modulus. Liu [13] proposed a gradient-based analytical method to calculate the sensitivity of the frequencies and mode shapes with respect to fibre volume fractions and fibre orientations of T-shape and square composite laminated plates. The gradient-based sensitivity analysis (SA) method falls in the category of the local SA (LSA) which concentrates on measuring the local effects of the variations in input parameters on model outputs. By contrast, Dey et al. [14] presented a global sensitivity analysis (GSA) approach based on random sampling-high dimensional model representations for composite plates. They investigated the influence of fibre-orientation angle, elastic modulus and mass density on natural frequencies of a composite plate, and found that the first three natural frequencies are most sensitive to ply-orientation and least sensitive to elastic modulus.

The aforementioned research, except the work by Allegri et al. [11], was restricted to either UQ or SA (mainly LSA) of dynamic responses in FRP components and the uncertainty modelling started from the ply level. Little attention has been paid to UQ and/or GSA of dynamic responses of full-scale civil engineering FRP structures. Specifically, UQ can be used to quantify the uncertainty in dynamic responses propagated from uncertain parameters whilst the GSA is an extension of UQ that allows for determining the contributions of uncertain parameters to the resulting uncertainty of dynamic responses. In structural engineering design, FRP profiles are commonly used, including I, channel and box sections, as well as custom shapes. The full-section properties of FRP profiles, normally obtained from manufacturers, are usually needed in the design. Therefore, to perform UQ and GSA of dynamic responses for actual FRP structures, it is more practical to use the effective properties of FRP profiles and start the uncertainty modelling from the component level.

This study focuses on UQ and GSA of dynamic responses of a full-scale 16.90 m long all-FRP footbridge whereby the uncertainty of input parameters is modelled at the component level. MCS has been extensively employed in the literature to solve UQ and GSA problems since it is intuitive and straightforward to implement and it is generally applicable to a variety of problems. However, MCS requires a large number of model evaluations to ensure the convergence with an acceptable accuracy, which severely hinders its wider applications to large-scale engineering structures. For instance, it was reported that the MCS implementation of UQ for a full-scale concrete-filled tubular arch bridge spanning 90 m took around 45 days on a DELL desktop machine with Pentium (R) D CPU 2.80 GHz [15]. When adopting MCS procedure, GSA is computationally more expensive than UQ since it requires calculation of the partial variances in addition to the computation of total variance. By contrast, the PCE method [16,17], as a surrogate model to represent the probabilistic response as a series expansion of orthogonal polynomials of the random variables, has great capability to model highly complex systems with low computational cost [18]. In particular, once the PCE model is established, the tasks of both UQ and GSA can be efficiently performed within the fast-to-run surrogate model rather than the time-consuming original model. The statistical moments (e.g. mean and variance) of target responses as well as the sensitivity indices of uncertain parameters can then be analytically calculated by post-processing the PCE coefficients. Therefore, the PCE method is especially useful for the UQ and GSA of full-scale FRP structures.

This paper aims to determine the effects of the uncertainties in mechanical properties of FRP components on the dynamic properties (natural frequencies and modal masses corresponding to unity-scaled mode shape) and vibration response of an actual all-FRP footbridge. The work: 1) presents a straight-forward and computationally economical numerical approach for UQ and GSA in full-scale FRP composite structures and 2) provides a comprehensive numerical insight into the effects of mechanical uncertainties for the longitudinal and transverse homogenised elastic modulus and the shear modulus for structural components. It is assumed that design values of mechanical properties of FRP components represent the mean values. Since the research is focused on the effects of uncertainties in FRP components, the pedestrian load is assumed to be deterministic as specified in ISO 10137 [19] for the purpose of evaluating vibration serviceability limit state. The methodology presented in the paper, using an example of a FRP footbridge subjected to dynamic loading by a pedestrian, can be generalised to structures subjected to any static or dynamic loads.

Following this introductory section, Sections 2 and 3 introduce the method for vibration response analysis of footbridges and the PCE-based UQ and GSA methods, respectively. Section 4 details the development of the nominal finite element (FE) model of a full-scale all-FRP footbridge and dynamic analysis. In Section 5, the UQ and GSA of dynamic properties and vibration response are presented. Conclusions are drawn in Section 6.

2. Vibration response of footbridges

For a slender footbridge with well separated vibration modes, vibration serviceability criteria specified in design standards routinely require the estimation of the vertical vibration response caused by an average single pedestrian. One of the first five harmonics of the pedestrian's walking force is assumed to match one of the structural natural frequencies [20–22]. In such an analysis, the walking force is assumed to be a harmonic force and one (most relevant) vibration mode of the structure is modelled as a single degree of freedom (SDOF) system. The calculated response at the antinode of the relevant mode shape is then compared with predefined vibration limits (typically separating a region of acceptable from unacceptable vibration). More

advanced design guidelines also require assessment of the vibration performance to crowd loading [23,24]. The vibration response in this case is estimated by multiplying the response to an average single person excitation by a suitable factor that is a function of the number of pedestrians present on the bridge at any one time and, in some cases, the damping ratio of the relevant mode of vibration. The selection of load model (i.e. single person loading or multiple-person loading) depends on the purpose and use of the bridge as well as its geometry (e.g. the deck width) [25].

The formulation for calculating the vertical vibration response due to a single person loading is presented here as it is most relevant for the footbridge considered in this paper. The bridge is modelled as a SDOF model with modal mass m_s, natural frequency f_s, damping ratio ζ_s and unity-normalised mode shape $\phi(x)$, where x represents the position along the bridge longitudinal axis. A harmonic force model traversing the bridge at a constant speed $v_w = f_w l_w$ is used to represent a walking person [19]. Step frequency f_w is assumed to be equal to f_s/i (i = 1, 2, 3, 4, 5) to generate the worst-case, and physically feasible, response in resonance by one of the first five forcing harmonics, whilst l_w represents the step length. The force representing pedestrian, therefore, is [19]

$$F(t) = \gamma G_0 \sin(2\pi f_s t) \tag{1}$$

where G_0 is the weight of the pedestrian and γ is the dynamic loading factor which represents the amplitude of the dynamic force normalised by G_0.

The equation governing the motion of the footbridge is [26]

$$\ddot{y}_s(t) + 2\zeta_s \omega_s \dot{y}_s(t) + \omega_s^2 y_s(t) = \frac{F(t)}{m_s}\phi(x) \tag{2}$$

where $y_s(t)$ is the modal displacement of the bridge and $\omega_s = 2\pi f_s$ is the circular natural frequency of the bridge. $x(t) = v_w t$ describes the position of the pedestrian along the bridge. Dots denote the derivatives with respect to time.

3. Uncertainty quantification and global sensitivity analysis using PCE

3.1. Formulation of PCE

PCE is a spectral decomposition technique that allows users to map the input-output relationship of a physical system by projecting it onto a basis of orthogonal polynomials with respect to the probability measure of input random variables [27]. Consider a physical system $\mathcal{M}(\bullet)$, which is usually an expensive-to-run black-box function, with a set of random variables $\boldsymbol{\xi} = \{\xi_1, \xi_2, ..., \xi_d\}$. The PCE representation of the target model can be expressed as

$$\begin{aligned}\mathcal{M}(\boldsymbol{\xi}) = \beta_0\Psi_0 + \sum_{\alpha_1=1}^{\infty}\beta_{\alpha_1}\Psi_1(\xi_{\alpha_1}) + \sum_{\alpha_1=1}^{\infty}\sum_{\alpha_2=1}^{\alpha_1}\beta_{\alpha_1\alpha_2}\Psi_2(\xi_{\alpha_1}, \xi_{\alpha_2}) \\ + \sum_{\alpha_1=1}^{\infty}\sum_{\alpha_2=1}^{\alpha_1}\sum_{\alpha_3=1}^{\alpha_2}\beta_{\alpha_1\alpha_2\alpha_3}\Psi_3(\xi_{\alpha_1}, \xi_{\alpha_2}, \xi_{\alpha_3}) + \cdots\end{aligned} \tag{3}$$

or in compact form

$$\mathcal{M}(\boldsymbol{\xi}) = \sum_{\boldsymbol{\alpha}\in\mathbb{N}^d}\beta_{\boldsymbol{\alpha}}\Psi_{\boldsymbol{\alpha}}(\boldsymbol{\xi}) \tag{4}$$

where $\mathbb{N}^d$ is the set of d-tuples of natural numbers; $\boldsymbol{\alpha} = \{\alpha_1, ..., \alpha_i, ..., \alpha_d\}$ are an d-dimensional indices; α_i refers to the degree of the ith random variable; $\beta_{\boldsymbol{\alpha}}$ are the PCE coefficients; and $\Psi_{\boldsymbol{\alpha}}(\boldsymbol{\xi})$ are the multivariate polynomials of order $\boldsymbol{\alpha}$. For practical implementation, the PCE with an infinite number of terms defined in Eq. (4) needs to be truncated to a finite degree p, yielding the following approximation

$$\mathcal{M}(\boldsymbol{\xi}) \approx \sum_{\boldsymbol{\alpha}\in\mathcal{A}^{p,d}}\beta_{\boldsymbol{\alpha}}\Psi_{\boldsymbol{\alpha}}(\boldsymbol{\xi}), \quad \mathcal{A}^{p,d} \equiv \{\boldsymbol{\alpha}\in\mathbb{N}^d : ||\boldsymbol{\alpha}||_1 \le p\} \tag{5}$$

where

$$||\boldsymbol{\alpha}||_1 = \sum_{i=1}^{d}\alpha_i \tag{6}$$

As a result, the total number of terms retained in the above truncated PCE is

$$K + 1 = \frac{(d+p)!}{d!p!} \tag{7}$$

The multivariate polynomials $\Psi_{\boldsymbol{\alpha}}(\boldsymbol{\xi})$ are formulated by the tensor product of the univariate ones

$$\Psi_{\boldsymbol{\alpha}}(\boldsymbol{\xi}) = \prod_{i=1}^{d}\psi_{\alpha_i}(\xi_i) \tag{8}$$

where $\psi_{\alpha_i}(\xi_i)$ are univariate polynomials that are orthogonal with respect to the probability distribution $\rho(\xi_i)$. The univariate orthogonal polynomials $\psi(\xi)$ satisfy the well-known three-term recurrence relation

$$\begin{aligned}&\psi_{h+1}(\xi) = (\xi - a_h)\psi_h(\xi) - b_h\psi_{h-1}(\xi), \quad h = 0, 1, 2, ... \\ &\psi_{-1}(\xi) = 0, \quad \psi_0(\xi) = 1\end{aligned} \tag{9}$$

for which the recurrence coefficients are determined by the Darboux's formulae [28]

$$a_h = \frac{\langle \xi\psi_h, \psi_h\rangle}{\langle \psi_h, \psi_h\rangle}, \qquad h = 0, 1, 2, ... \tag{10}$$

and

$$b_h = \begin{cases}\langle \psi_0, \psi_0\rangle, & h = 0, \\ \frac{\langle \psi_h, \psi_h\rangle}{\langle \psi_{h-1}, \psi_{h-1}\rangle}, & h = 1, 2, ...\end{cases} \tag{11}$$

where $\langle \bullet, \bullet\rangle$ stands for the inner product operator. As shown in Eqs. (10) and (11), the recurrence coefficients of a univariate orthogonal polynomial are uniquely determined by its probability distribution. For most standard probability distributions (such as, uniform, normal and gamma), the recurrence coefficients are known analytically, while for other probability distributions (such as, Weibull and Rayleigh) without analytical recurrence coefficients, the discretisation method can be used to determine these terms. Further details on the calculation of the recurrence coefficients are available elsewhere [29].

The least-square minimisation is employed here to estimate the PCE coefficients because of its efficiency for high dimensional problems. Let $\{\boldsymbol{\xi}_t\}_{t=1}^n$ be n samples of random variables and $\{y_t = \mathcal{M}(\boldsymbol{\xi}_t)\}_{t=1}^n$ be the corresponding target responses, and then the PCE coefficients $\hat{\boldsymbol{\beta}}_{\boldsymbol{\alpha}}$ can be estimated by solving the following least-square minimisation problem

$$\hat{\boldsymbol{\beta}}_{\boldsymbol{\alpha}} = \arg\min_{\beta_{\boldsymbol{\alpha}}\in\mathbb{N}^{K+1}}\sum_{t=1}^{n}\left[y_t - \sum_{\boldsymbol{\alpha}\in\mathcal{A}^{p,d}}\beta_{\boldsymbol{\alpha}}\Psi_{\boldsymbol{\alpha}}(\boldsymbol{\xi}_t)\right]^2 \tag{12}$$

3.2. Analytical calculation of statistical characteristics

In statistics, statistical moments are used to characterise a variable's probability distribution. The most common statistical moments are mean, which is a measure of the central tendency, and variance (or standard deviation), which characterises the variability around the mean value. For a response that follows a distribution (such as uniform and normal) that is fully defined by two parameters, the mean and variance are sufficient for the determination of its probability distribution.

Generally speaking, the calculation of statistical characteristics of system responses involves complex high-dimensional integrals. The use of the PCE surrogate model enables an efficient evaluation of the response statistics. More specifically, the mean μ and variance σ^2 can be analytically calculated by post-processing the PCE coefficients

$$\mu = \beta_0 \tag{13}$$

$$\sigma^2 = \sum_{j=1}^{K} \beta_j^2 \tag{14}$$

3.3. Analytical implementation of global sensitivity analysis

GSA is a powerful scheme for performing sensitivity analysis, allowing for reliable assessment of the relative importance of uncertain parameters based on their contributions to the variance of the model output. It can be used for assessing the influence of the individual input parameters over the whole input space on model responses as well as their combined effects. The GSA is based on functional analysis of variance (ANOVA), that is, the total output variance can be decomposed into a collection of partial variances induced by the effects of individual inputs and the interaction effects. Specifically, the decomposition of the total variance of model output can be expressed as [30]

$$V = \sum_{1\le i\le d} V_i + \sum_{1\le i<j\le d} V_{i,j} + \sum_{1\le i<j<k\le d} V_{i,j,k} + \cdots + V_{1,2,\ldots,d} \tag{15}$$

with

$$\begin{aligned} V &= \mathbb{V}(y) \\ V_i &= \mathbb{V}(\mathbb{E}(y|\xi_i)) \\ V_{i,j} &= \mathbb{V}(\mathbb{E}(y|\xi_i, \xi_j)) - V_i - V_j \\ V_{i,j,k} &= \mathbb{V}(\mathbb{E}(y|\xi_i, \xi_j, \xi_k)) - V_{i,j} - V_{i,k} - V_{j,k} - V_i - V_j - V_k \\ &\cdots \end{aligned} \tag{16}$$

where $\mathbb{E}(\bullet)$ and $\mathbb{V}(\bullet)$ denote the expectation and variance operators, respectively. y and $\boldsymbol{\xi}$ are the output and input variables, respectively.

The variance-based sensitivity indices are defined as the ratios of the partial variances to the total variance. Within the framework of GSA, of particular interest are the first-order and total sensitivity indices, which are expressed as

$$S_i = \frac{V_i}{V} \tag{17}$$

and

$$S_{Ti} = 1 - \frac{V_{-i}}{V}, \tag{18}$$

respectively, where $V_{-i} = \mathbb{V}(\mathbb{E}(y|\boldsymbol{\xi}_{-i}))$, in which $\boldsymbol{\xi}_{-i} = \{1,\ldots,\xi_{i-1},\xi_{i+1},\ldots,\xi_d\}$ denotes all inputs $\boldsymbol{\xi}$ except ξ_i. The first-order sensitivity index S_i measures the contribution to the total variance accounted for by the ith input alone, whereas the total sensitivity index S_{Ti} evaluates the total contribution accounted for by all the ith input-related terms. The difference between them is that the latter takes into account the interaction effects among the inputs while the former does not.

Due to the orthogonal nature of the basis functions of PCE, the variance-based sensitivity indices can be computed analytically by simply post-processing PCE coefficients [31], such that

$$\widehat{S}_i = \frac{\sum_{k\in\mathcal{L}_i} \beta_k^2 \langle \Psi_k, \Psi_k \rangle}{\sum_{k=1}^{K} \beta_k^2 \langle \Psi_k, \Psi_k \rangle} \tag{19}$$

$$\widehat{S}_{Ti} = \frac{\sum_{k\in\mathcal{L}_{Ti}} \beta_k^2 \langle \Psi_k, \Psi_k \rangle}{\sum_{k=1}^{K} \beta_k^2 \langle \Psi_k, \Psi_k \rangle} \tag{20}$$

where index sets $\mathcal{L}_i = \{k \in \mathcal{A}^{p,d}: k_i > 0, k_\ell = 0, \ell \neq i\}$; and $\mathcal{L}_{Ti} = \{k \in \mathcal{A}^{p,d}: k_i > 0\}$.

3.4. Implementation of the PCE-based UQ and GSA

A flowchart for the proposed PCE-based UQ and GSA method is shown in Fig. 1. It comprises of main stages as follows:

(I) Sobol sequence-based experimental design [32], which has a desirable low-discrepancy (space-filling) property, is used to generate input points based on parameter probability distributions. Note that Sobol points uniformly fall in the unit hypercube $[0, 1]^d$, while the structural parameters follow specific distributions. Therefore, before entering inputs into a numerical model of the system under consideration (e.g. the FE model of the footbridge considered in this paper), Sobol points are transformed into the physical space of structural parameters based on the cumulative probability equality principle.

(II) Subsequently, each transformed input is entered into the numerical model to calculate the associated dynamic properties and vibration response.

(III) The PCE items can be determined based on an adopted model order and parameters' probability distributions. Then the least-square estimator is used to calculate the PCE coefficients. Once the PCE model is built, the explicit expressions of the relationship between random parameters and dynamic responses are attained. The statistical characteristics (mean and variance) of dynamic responses and sensitivity indices of mechanical parameters are then analytically obtained using Eqs. (13) and (14) and Eqs. (19) and (20), respectively.

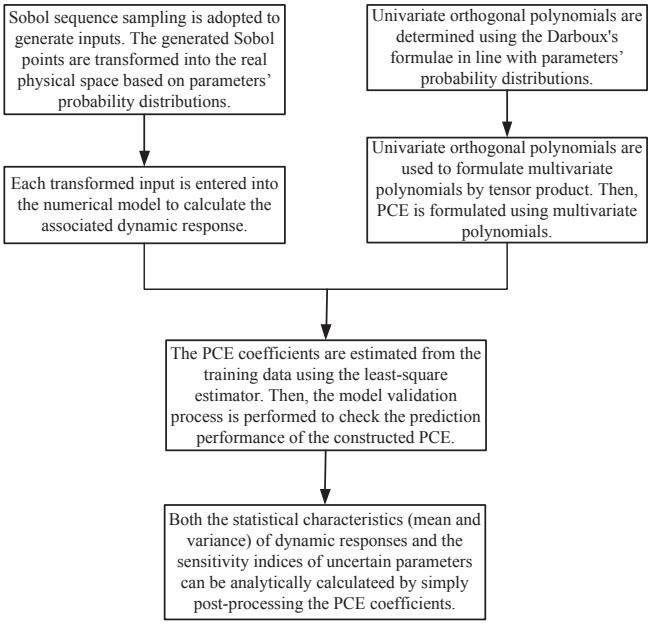

Fig. 1. Flowchart of PCE-based UQ and GSA.

4. Dynamic analysis of a full-scale all-FRP footbridge

4.1. Bridge description

An all-FRP, simply supported, composite footbridge shown in Fig. 2 is considered. The bridge comprises of a single span FRP square box girder that is 0.78 m wide, 0.78 m deep and 16.90 m long. The handrails are made of FRP sections and there is a layer of asphalt surfacing. The girder consists of the Advanced Composites Construction System (ACCS) panels made of glass fibre-polyester matrix pultruded material and 3-way connectors, as shown in Fig. 2b. Within the girder are five diaphragms, evenly spaced along the bridge, connected to the sides of the box. The primary vertical members of the handrail system are made of 1910 mm high 3-way connectors placed every 845 mm. The horizontal elements of tube sections have a diameter of 57.16 mm and thickness of 3.17 mm. The secondary elements in the vertical direction are tube sections have a diameter of 38.2 mm and thickness of 3.17 mm, with five placed evenly between each primary upright. The handrails are attached to the side of the bridge by two steel bolts per post. The

(a) (b)

Fig. 2. Photographs of the footbridge: (a) side view; (b) square box cross-section.

handrails extend 0.845 m beyond the length of the girder so that the end posts are fixed to the ground. The total mass of the modelled bridge is 1847 kg.

4.2. Nominal finite element model

A nominal finite element (FE) model was created using Abaqus/Standard software [33] based on the design of the bridge and geometry measurements taken on site. Fig. 2b shows geometry of the section in the FE model. The panel was modelled with 4-node reduced integration shell element (element ID S4R) whilst the 3-way connectors and FRP tube sections were all modelled as 2-node linear beam elements (element ID B31). The orthotropic shell elements in the ACCS panels were assigned material properties provided in Table 1. The 3-way connectors used in the corners of the box and for the handrail posts were assigned isotropic properties given in Table 2, as their location means their longitudinal characteristics dominate their contributions. Similarly, the handrail tube beam elements were also modelled as isotropic elements with properties listed in Table 2.

A point mass of 0.721 kg representing each of 84 steel bolts was added at the points of handrail attachment to the box girder. The asphalt surfacing was modelled using a uniform mass of 30 kg/m^2 added to the top panel of the girder. The diaphragm sections were rigidly constrained to the inner side surfaces of the box. The handrails were rigidly constrained to the sides of the beam. The bases of the end handrail posts that are connected to the ground were fixed in all directions. The box was simply supported 422.5 mm from each end of the beam. Pinned-roller supports were assigned along this line at both ends. To provide longitudinal restraint, without influencing the lateral bending stiffness, an additional restraint at the centre line of the beam was applied at one end at this point as well. In total there are 27,104 elements and 30,703 nodes. A rendered image of the FE model is shown in Fig. 3.

4.3. Dynamic responses of the nominal footbridge

This section presents the dynamic parameters and vertical vibration response to a pedestrian for the nominal footbridge.

4.3.1. FE modal analysis

The dynamic properties of the first three flexural modes of the box girder are calculated using modal analysis and they are summarised in Table 3. The modal masses correspond to the unity-scaled mode shapes shown in Figs. 4–6.

Table 2
Material properties for 3-way connectors and FRP tubes.

	3-way connectors	FRP tubes
Density (kg/m^3)	1950	1800
Young's modulus (GPa)	32	20
Poisson's ratio	0.35	0.35

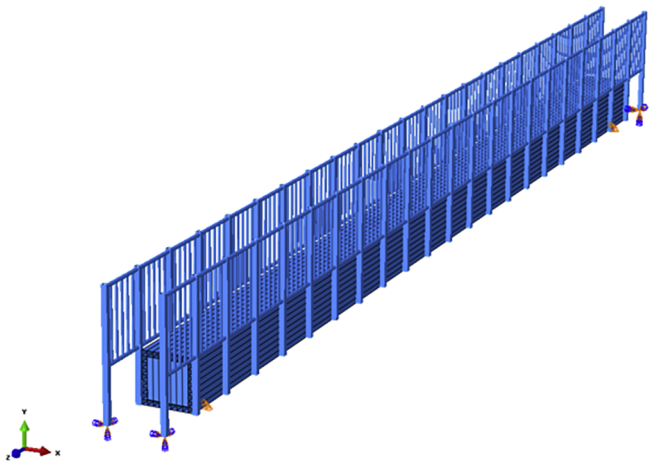

Fig. 3. FE model of the footbridge.

Table 3
Modal parameters of the nominal bridge.

No.	Description	Frequency (Hz)	Modal mass (kg)
1	1st lateral bending	4.31	607
2	1st vertical bending	4.90	862
3	2nd vertical bending	15.82	907

Table 1
Material properties for ACCS panels.

Density (kg/m^3)	Longitudinal elastic modulus (GPa)	Transverse elastic modulus (GPa)	Shear moduli (GPa)	Poisson's ratios
1950	21.6	10	3	0.35

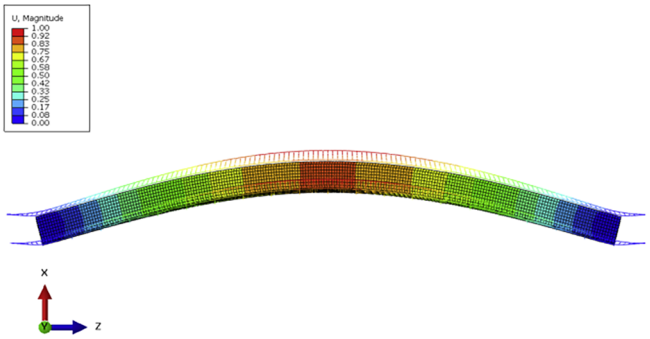

Fig. 4. 1st lateral bending mode (Top view).

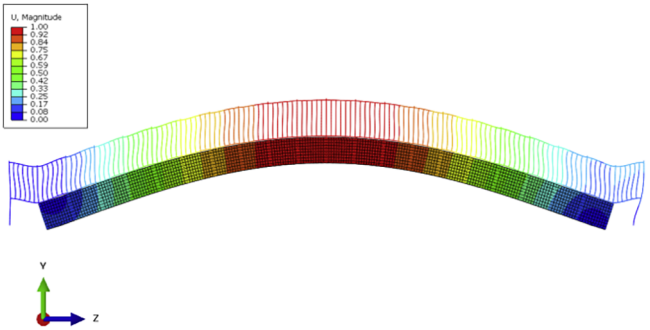

Fig. 5. 1st vertical bending mode (Side view).

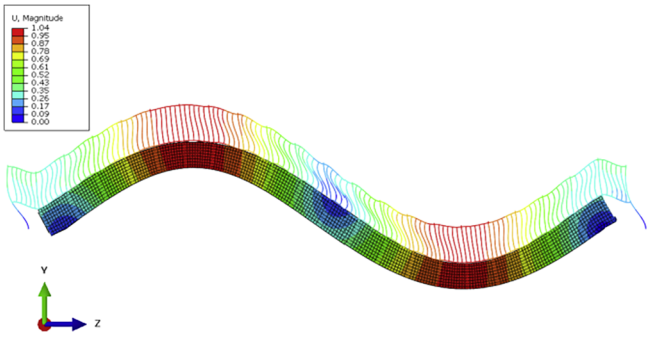

Fig. 6. 2nd vertical bending mode (Side view).

4.3.2. Analysis of vertical vibration due to walking excitation

The vertical vibration modes of the bridge are well separated, and only the first vertical mode is located in the frequency range of the first five harmonics of the walking force, ranging from 1.2 Hz to 12.0 Hz [19]. Hence, the first vertical mode only is of interest here. The bridge is modelled as a SDOF model having modal mass of 862 kg and natural frequency f_s of 4.9 Hz. The damping is assumed to be proportional damping. The damping ratio is calculated to be 2.4% by using the Eq. (21),

$$\zeta_s = c_1 \frac{\omega_s}{2} + \frac{c_2}{2\omega_s} \tag{21}$$

where $\omega_s = 2\pi f_s$, $c_1 = 0.0005$ and $c_2 = 1.0$. c_1 and c_2 are empirical values from FRP footbridges of the same type [34].

The footbridge under consideration is narrow and located in a sparsely populated area. Therefore, the most relevant pedestrian loading scenario is a single pedestrian walking at 2.45 Hz to excite the resonance by the second harmonic of the force.

The pedestrian is assumed to have weight $G_0 = 700$ N and step length of $l_w = 0.71$ m [35]. The step frequency is $f_w = 2.45$ Hz. The walking speed is $v_w = f_w l_w = 1.74$ m/s, whilst $\gamma = 0.1$ in Eq. (1).

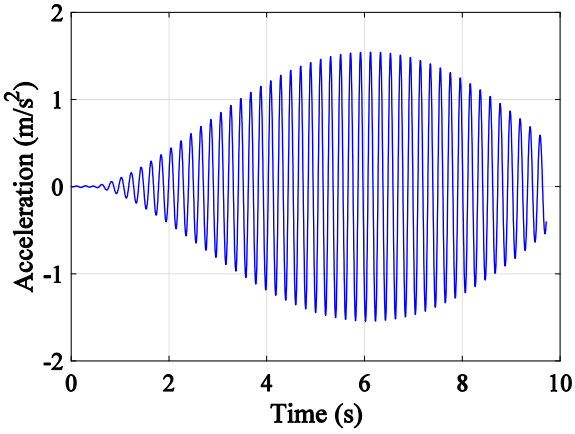

Fig. 7. Acceleration at the midspan of the nominal footbridge.

Therefore, the nominal walking force is $F = 70\sin(9.8\pi t)$ N [19]. The vertical acceleration of the footbridge is calculated from Eq. (2) using the Newark-β numerical integration method [36] with time step of 0.005 s. The resulting response, with a peak value of 1.54 m/s^2, is shown in Fig. 7.

5. Influence of mechanical uncertainties on dynamic responses

This section investigates the impact of the uncertainties in mechanical properties of the FRP components on the dynamic properties, vibration response and vibration serviceability assessment of the footbridge.

5.1. Characterisation of mechanical uncertainties

The main structural components are the ACCS panels and 3-way connectors. Hence, variations of the mechanical properties of these two components are considered only. The uncertain quantities are the longitudinal and transverse elastic modulus and shear modulus of the panel, and the Young's modulus of the 3-way connector. The Poisson's ratio for the panels and 3-way connectors is assumed to be constant. The mass density is also treated as constant since the proportions of the fibre and matrix in pultruded profile materials are straight forward to control during the pultrusion process. The specifications for the four uncertain mechanical parameters are listed in Table 4, based on data available in [37–43]. The mean values stated in the table are those used in the nominal FE model. The coefficient of variation (COV) is assumed to be 10% [5,44]. In addition, it is assumed that the random mechanical properties follow Weibull distribution, which is most commonly used for composites [6,42,44] and they are assumed to be mutually independent. Additionally, the perfect correlation is assumed for members of the same type (i.e. all members of the same type possess the same random value for each material property). Note that the PCE-based approach can also be used for the case with correlated random variables [45,46].

5.2. Uncertainty quantification of dynamic responses

In this section, the UQ in the dynamic properties and vibration response of the footbridge with uncertain mechanical properties given in Table 4 is implemented by following the procedures for the PCE-based UQ method described in Section 3.4. The model order p is set to 2 and the sample size for each mechanical property is set to 600. In general, different PCE model orders can be utilized to fit different output variables. The selection of model order and sample size for construction of PCE models is explored in Section 5.4. MCS is conducted and the results are used as benchmark solutions for the verification of the PCE-based

Table 4
Statistics of mechanical properties of FRP components [37–43].

Component	Mechanical property	Distribution	Mean (GPa)	COV (%)
Panel	Longitudinal elastic modulus (E_L)	Weibull	21.6	10
	Transverse elastic modulus (E_T)	Weibull	10	10
	Shear modulus (G_S)	Weibull	3	10
3-way connector	Young's modulus (E_Y)	Weibull	32	10

UQ method. The sample size for the MCS is set to 10,000, based on [47,48].

5.2.1. Modal parameters

Following the procedures for the PCE-based UQ method summarised in Section 3.4, Sobol sequence-based experimental design was first carried to generate samples for the four uncertain mechanical properties. Modal analysis was then performed on the FE model of the footbridge for each set of samples, which resulted in calculation of unity-scaled mode shapes, natural frequencies and modal masses.

It is found that for every set of samples, the first lateral, first vertical and second vertical modes of the deck preserve (qualitatively) the same global shape as observed in the nominal bridge mode, but they have slightly different frequencies and modal masses. Note that modal mass represents the physical mass weighted by the square of the magnitude of the relevant mode shape. This bridge has an approximately uniformly distributed physical mass, and therefore any variation in the calculated modal mass is due to the variation in the mode shape. The damping ratio for each sampled data point is calculated using Eq. (21) and the circular frequency for each sampled data point.

Based on the least-square estimator, the PCE coefficients for natural frequencies and modal masses were estimated and subsequently their means and standard deviations were analytically obtained using Eqs. (13) and (14). The results are shown in Figs. 8 and 9, along with their COVs. They are also compared with their counterparts from MCS. The excellent agreement between the two methods demonstrates high accuracy of the PCE-based method. The results show that a COV of 10% for the four mechanical parameters leads to the COVs of 3.37%, 2.92% and 3.07% for the natural frequencies of the first lateral, first vertical and second vertical modes, respectively. By contrast, the resultant COVs of the modal masses of the first lateral, first vertical and second vertical modes are 2.98%, 0.04% and 0.61%, respectively. These variations in modal parameters are due to the variations in the relative stiffness of the structural elements. The first lateral mode has the largest COV of modal mass while the first vertical mode has the smallest COV of modal mass. This is because the mode shape of the first lateral mode includes the most contribution from the handrails while the first vertical mode contains the least. The participation of the handrails, which are much less stiff than the box girder, in the modal motion of the whole bridge is affected more by the changes in the stiffness distribution of the bridge elements.

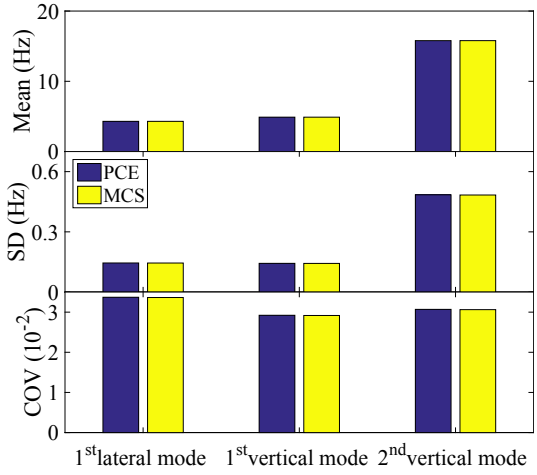

Fig. 8. Statistical characteristics of natural frequencies.

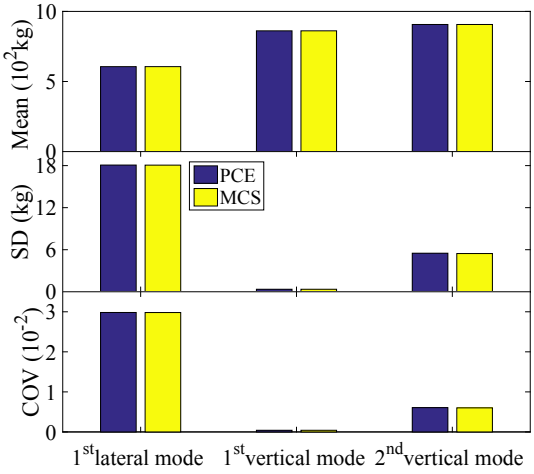

Fig. 9. Statistical characteristics of modal masses.

5.2.2. Vibration serviceability assessment

This section presents the effects of the uncertainties in mechanical properties of FRP components on the vibration serviceability assessment of the footbridge excited in resonance by a single pedestrian. The pedestrian is modelled in the same way as described in Section 4.3.2. For each model realisation, the walking frequency is equal to half of the frequency of the first vertical mode.

For each set of samples of mechanical properties, the modal mass, frequency and damping ratio of the first vertical mode can be obtained using the methods presented in Section 5.2.1. Then, the vibration response was calculated in the same way for the nominal case. Likewise, the PCE-based UQ method was adopted to calculate the mean, standard deviation and COV of the absolute peak acceleration, resulting in values of 1.54 m/s^2, 0.014 m/s^2 and 0.93%, respectively (Fig. 10). This result indicates that the uncertainties in mechanical properties of FRP components have relatively small effects on the peak acceleration value. The statistical characteristics obtained by the PCE method match well those calculated by MCS, as shown in Fig. 10.

To put the results presented in the context of vibration serviceability evaluation of the bridge, vibration limits defined by Sétra guidelines [23] are used. Four comfort levels are defined based on the peak acceleration ranges: 0–0.5 m/s^2 is maximum comfort, 0.5–1 m/s^2 is mean comfort, 1–2.5 m/s^2 is minimum comfort and above 2.5 m/s^2 is unacceptable. It can be concluded that both the nominal footbridge response of 1.54 m/s^2 and its variations result in minimum comfort level for bridge users. Therefore, in this case study, variations in the mechanical properties of FRP elements did not result in changes in the comfort level due to the small variation in vertical vibration response. This conclusion might change once more sophisticated stochastic

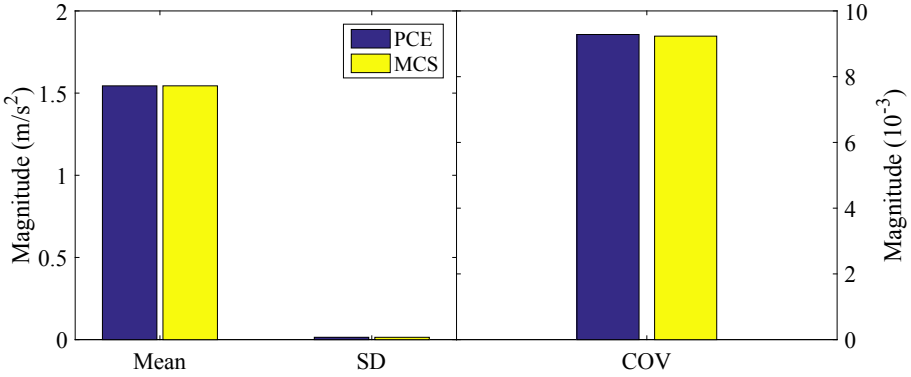

Fig. 10. Statistical characteristics of the absolute peak acceleration at the midspan of the bridge.

models for pedestrians and the non-resonance loading conditions are introduced into the framework analysis, which is the next step in our research.

5.3. Global sensitivity analysis of dynamic responses

Following the UQ, GSA is performed to assess the sensitivity of the dynamic properties and vibration response to uncertain parameters based on the formulas in Section 3.3. The GSA results lead to the following observations:

- For the natural frequencies, the longitudinal elastic modulus of the panel E_L is the most influential parameter while the transverse elastic modulus E_T has negligible influence. The elastic modulus of the 3-way connector E_Y is the second most influential parameter for the first lateral and first vertical natural frequencies, and the shear modulus of the panel G_S is the second most influential for the second vertical natural frequency (Fig. 11). One can observe that joint effects among parameters do not exist since there is almost no difference between the first-order and total sensitive indices S_i and S_{Ti}.
- The GSA results are different for modal masses compared to those for natural frequencies. For the first lateral and second vertical natural frequencies, the parameters E_L and G_S are dominant contributors and the remaining two parameters have negligible influence. For the first vertical natural frequency, the parameter G_S exhibits the most significant influence, followed by E_Y, E_T and E_L, respectively. The interaction effects among parameters are not significant (Fig. 12), as was the case for natural frequencies.
- E_L influences the peak acceleration response most. E_Y ranks the second and the remaining parameters are of little importance

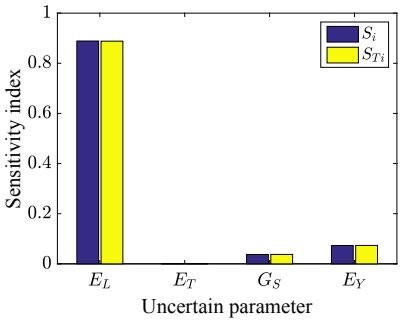

(a) 1st lateral natural frequency

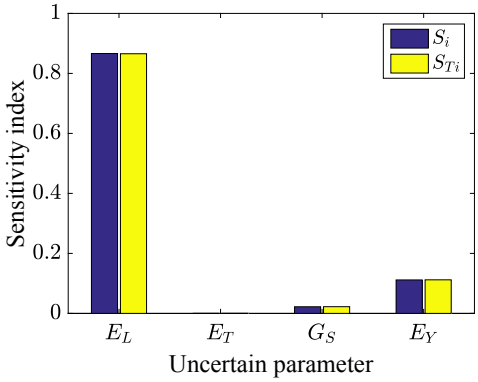

(b) 1st vertial natural frequency

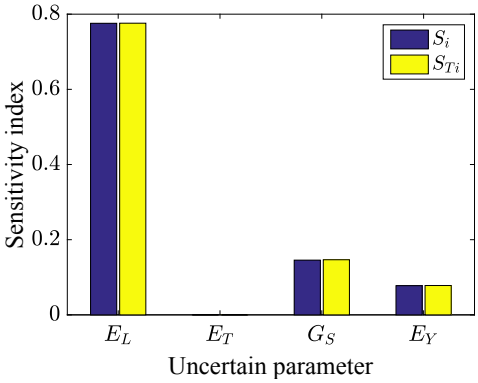

(c) 2nd vertical natural frequency

Fig. 11. Global sensitivity of the first three natural frequencies to uncertain parameters.

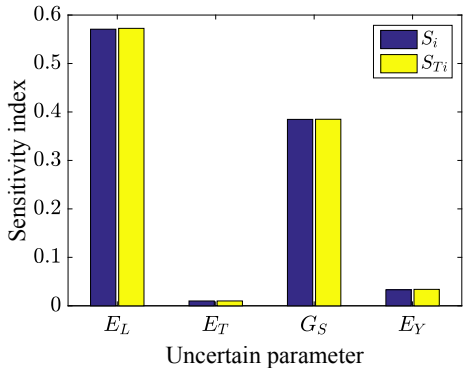

(a) 1st lateral modal mass

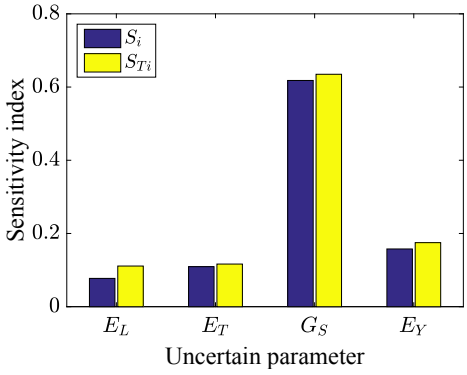

(b) 1st vertical modal mass

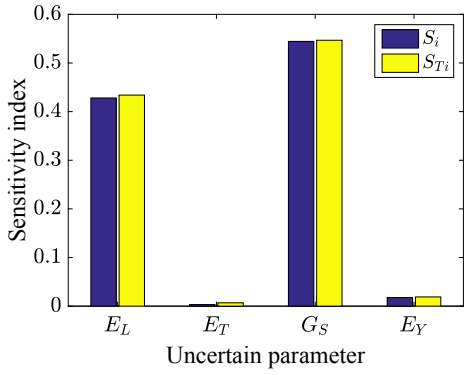

(c) 2nd vertical modal mass

Fig. 12. Global sensitivity of the first three modal masses to uncertain parameters.

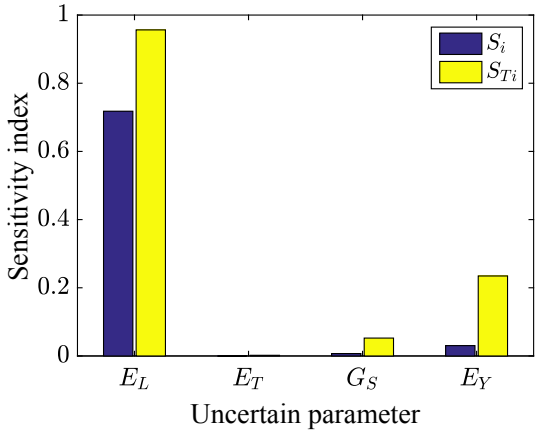

Fig. 13. Global sensitivity of the absolute peak acceleration to uncertain parameters.

(Fig. 13). Different from the previous results, the joint effects of the parameters on the absolute peak acceleration is substantial, as indicated by the pronounced discrepancy between their first-order and total sensitivity indices S_i and S_{Ti}.

Overall, the longitudinal elastic modulus and shear modulus of the panel are the most influential parameters for dynamic properties and vibration response, and the influences of the transverse elastic modulus and the elastic modulus of the 3-way connector are negligible. Therefore, substantial attention should be paid to the accurate characterisation of the statistics of the two dominant parameters since they mainly account for the variability in the dynamic responses.

5.4. Investigation of model order and sample size

The model order (p) and sample size (n) are two crucial factors that influence the accuracy of PCE. The former determines the total number of PCE terms, whereas the latter reflects how many samples should be generated for PCE construction. Eq. (7) indicates the number of the PCE terms will grow exponentially with model order. For four random variables, the 1-, 2-, 3-, and 4-order PCEs have a total number of 5, 15, 35, and 70 terms, respectively. These four model orders are considered here. The sample size ranges from 100 to 1000 with an increment of 10, resulting in a total of 91 sample cases.

The root mean square relative error (RMSRE)

$$\mathrm{RMSRE} = \sqrt{\frac{1}{2}\left[\left(\frac{\mathrm{S}_{\mathrm{PCE}}^{\mathrm{Mean}} - \mathrm{S}_{\mathrm{MCS}}^{\mathrm{Mean}}}{\mathrm{S}_{\mathrm{MCS}}^{\mathrm{Mean}}}\right)^2 + \left(\frac{\mathrm{S}_{\mathrm{PCE}}^{\mathrm{SD}} - \mathrm{S}_{\mathrm{MCS}}^{\mathrm{SD}}}{\mathrm{S}_{\mathrm{MCS}}^{\mathrm{SD}}}\right)^2\right]} \tag{22}$$

where S_{MCS} and S_{PCE} represent the MCS-estimated and PCE-derived statistical characteristics, respectively. RMSRE is used to evaluate the performance of the PCE method. A smaller value of RMSRE indicates better performance of the method. The results shown in Figs. 14–16 suggest that:

- Overall, the accuracy of PCE for UQ increases with increasing sample size but it becomes stable after a certain sample size, for example 600 samples for this study.
- Among the four model orders, the first order case exhibits the worst performance. This is due to the fact that the first order PCE is a linear model, which fails to map the nonlinear relationship between random parameters and dynamic responses.
- The higher order PCE will not necessarily lead to better performance due to possible overfitting issue. For example, for all three natural frequencies and absolute peak acceleration, the second order PCE

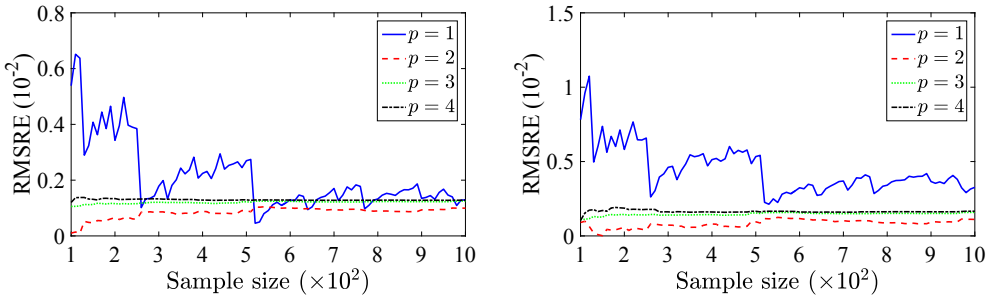

(b) 1st vertial natural frequency (c) 2nd vertical natural frequency

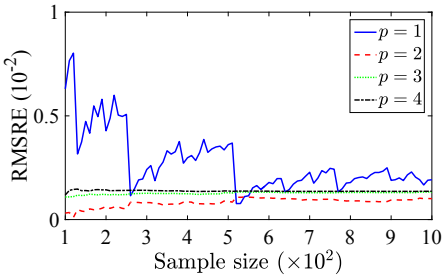

(b) 1st lateral natural frequency

Fig. 14. RMSRE of the modal frequencies under different model orders and sample sizes.

performs best as shown in Figs. 14 and 16.

- Although for all three modal masses the second order PCE does not generally maintain the better performance than the third and fourth order PCEs, the accuracy of the second order model is sufficiently high, as illustrated by its small RMSRE values. The increase of model order will lead to the exponential growth of the number of the PCE terms, which will result in more model evaluations for determining the PCE coefficients. Therefore, selecting the lowest order model suitable for problem under consideration is preferable. Due to the consistently good performance of second order PCE, this model order is used in this study for UQ of dynamic responses.
- The UQ performance of PCE is different for different target dynamic responses. For example, the second order PCE displays the best performance for the computation of the natural frequencies and absolute peak acceleration (Figs. 14 and 16), whereas, overall, the fourth order PCE demonstrates the best performance of the evaluation of modal masses (Fig. 15). For different dynamic responses, the underlying input-output relationship between the random parameters and dynamic responses can be different, such as weak or strong nonlinearity. This may explain the difference in UQ performance of PCE for different target dynamic responses.

It should be noted that it is not expected to have results of a full set of MCS to determine the model order and sample size. Instead, the

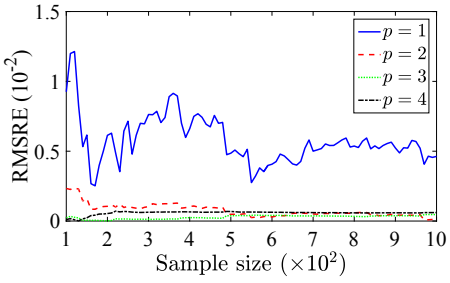

(a) 1st lateral modal mass

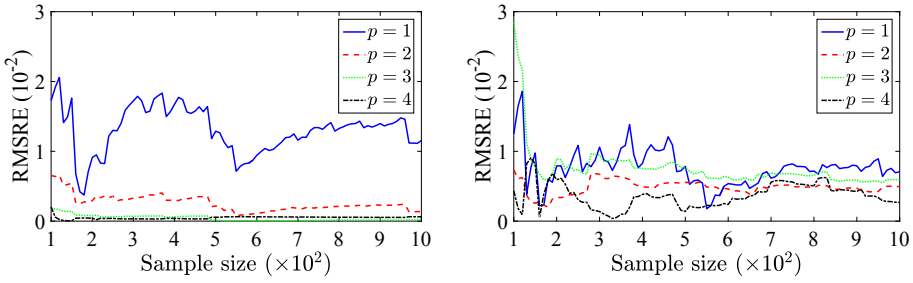

(b) 1st vertical modal mass (c) 2nd vertical modal mass

Fig. 15. RMSRE of the modal masses under different model orders and sample sizes.

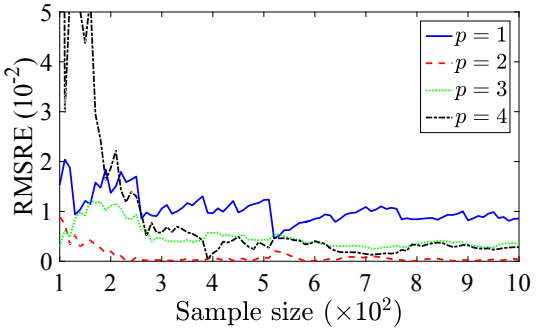

Fig. 16. RMSRE of the absolute peak acceleration under different model orders and sample sizes.

model validation process should be performed to check the prediction performance of the constructed PCE. The frequently used leave-one-out cross-validation (LOOCV) [49] for model diagnosis can be used for this purpose.

6. Conclusions

This paper presents a stochastic characterisation of the dynamic properties and vertical vibration response of a full-scale all-FRP bridge using the PCE-based UQ and GSA methods. The uncertain variables considered are the longitudinal and transverse elastic modulus and shear modulus of ACCS panels and the Young's modulus of 3-way connectors. The UQ and GSA are based on a nominal FE model for the FRP footbridge. The performance of the PCE-based UQ method is compared with the brute-force MCS. In addition, the effects of the model order and sample size on the PCE-based UQ performance are explored. The following conclusions can be drawn:

- The presented PCE-based UQ method enables the analytical determination of the stochastic characteristics of dynamic properties and vibration response using a small set of samples while maintaining accuracy comparable to MCS. The overwhelming advantage in computation effort over the MCS makes the PCE-based UQ method especially applicable to UQ problems in large-scale FRP structures.
- Overall, the uncertainties in mechanical properties of FRP components exert larger effects on natural frequencies than modal masses. For example, the COV of 10% for four mechanical parameters of FRP components leads to COVs of 3.37%, 2.92% and 3.07% for the natural frequencies of the first lateral, first vertical and second vertical modes, respectively. By contrast, the resultant COVs for the modal masses of these three modes are much smaller, at values 2.98%, 0.04% and 0.61%. The COVs for modal masses are found to be closely related to the participation of handrails in the modal motion of the bridge.
- The uncertainties in mechanical properties of FRP components have limited effects on vertical resonant responses to a pedestrian excitation modelled in a deterministic manner. For example, the COV of 10% for four mechanical parameters of FRP components can only lead to a COV of 0.93% for the absolute peak acceleration. This small variation in vertical vibration response has negligible effects on the vibration serviceability assessment for the FRP bridge. The proposed methodology opens the door for investigating the effects of uncertainties associated with pedestrian loading on the dynamic response.
- Overall, the longitudinal elastic modulus and shear modulus of the panel are the most influential parameters for dynamic properties and vibration responses, and the influence of the transverse elastic modulus and the elastic modulus of the 3-way connector are negligible. Therefore, it is reasonable to consider only the effects of the uncertainties in the two dominant parameters on the dynamic properties and vibration response of the full-scale FRP footbridge.
- The accuracy of PCE for UQ increases with sample size, up to a limit, 600 samples in this study. After this larger sample sizes only have a small influence on the accuracy. Using a higher-order PCE does not always give rise to better performance.

Acknowledgements

The authors acknowledge the support by the UK Engineering and Physical Sciences Research Council (Grant Number EP/M021505/1: Characterising dynamic performance of fibre reinforced polymer structures for resilience and sustainability) and insightful discussions with Prof. J. Toby Mottram at the University of Warwick and Dr. Jing Yang at Central South University. The data analysed in this paper can be reproduced using information provided in the paper.

References

[1] Živanović S, Feltrin G, Mottram JT, Brownjohn JMW. Vibration performance of bridges made of fibre reinforced polymer. Catbas FN, editor. Dynamics of civil structures, Volume 4. Springer International Publishing; 2014. p. 155–62.
[2] Wei X, Russell J, Živanović S, Mattram JT. Measured dynamic properties for FRP footbridges and their critical comparison against structures made of conventional construction materials. Compos Struct 2019. https://doi.org/10.1016/j.compstruct.2019.110956.
[3] Ellingwood BR. Toward load and resistance factor design for fiber-reinforced polymer composite structures. J Struct Eng 2003;129:449–58.
[4] Mottram JT. Fibre reinforced polymer structures: design guidance or guidance for designers. In: The 8th International Conference on Advanced Composites in Construction. Chesterfield, UK. 5–7 September, 2017.
[5] Sriramula S, Chryssanthopoulos MK. Quantification of uncertainty modelling in stochastic analysis of FRP composites. Composites Part A 2009;40:1673–84.
[6] ASCE. Pre-standard for load and resistance factor design (LRFD) of pultruded fibre reinforced polymer (FRP) structures. Reston VA: American Society of Civil Engineers; 2010.
[7] Piovan MT, Ramirez JM, Sampaio R. Dynamics of thin-walled composite beams: analysis of parametric uncertainties. Compos Struct 2013;105:14–28.
[8] Dey S, Mukhopadhyay T, Khodaparast HH, Adhikari S. Fuzzy uncertainty propagation in composites using Gram-Schmidt polynomial chaos expansion. Appl Math Model 2016;40:4412–28.
[9] Sepahvand K. Spectral stochastic finite element vibration analysis of fiber-reinforced composites with random fiber orientation. Compos Struct 2016;145:119–28.
[10] Awruch MDF, Gomes HM. A fuzzy α-cut optimization analysis for vibration control of laminated composite smart structures under uncertainties. Appl Math Model 2018;54:551–66.
[11] Allegri G, Corradi S, Marchetti M. Stochastic analysis of the vibrations of an uncertain composite truss for space applications. Compos Sci Technol 2006;66:273–82.
[12] Carvalho A, Silva T, Loja M. Assessing static and dynamic response variability due to parametric uncertainty on fibre-reinforced composites. J Compos Sci 2018;2:6.
[13] Liu Q. Analytical sensitivity analysis of frequencies and modes for composite laminated structures. Int J Mech Sci 2015;90:258–77.
[14] Dey S, Mukhopadhyay T, Adhikari S. Stochastic free vibration analysis of angle-ply composite plates – a RS-HDMR approach. Compos Struct 2015;122:526–36.
[15] Wan HP, Mao Z, Todd MD, Ren WX. Analytical uncertainty quantification for modal frequencies with structural parameter uncertainty using a Gaussian process metamodel. Eng Struct 2014;75:577–89.
[16] Wiener N. The homogeneous chaos. Am J Math 1938;60:897–936.
[17] Xiu D, Karniadakis G. The Wiener-Askey polynomial chaos for stochastic differential equations. SIAM J Sci Comput 2002;24:619–44.
[18] Fajraoui N, Marelli S, Sudret B. Sequential design of experiment for sparse polynomial chaos expansions. SIAM/ASA J Uncertainty Quantif 2017;5:1061–85.
[19] ISO. ISO 10137: 2007(E): bases for design of structures: Serviceability of buildings and walkways against vibrations. Geneva: International Organization for Standardization; 2007.
[20] CSA. Canadian highway bridge design code CAN/CSA-S6-00 Toronto, Canada: Canadian Standards Association; 2000.
[21] HA. Design manual for roads and bridges. Volume 1, Section 3: Loads for Highway Bridges (BD37/01). London (UK): Highway Agency; 2001.
[22] BSI. Mechanical vibration — evaluation of measurement results from dynamic tests and investigations on bridges. London, UK: British Standards Institution; 2004.
[23] Sétra. Footbridges. Assessment of vibrational behaviour of footbridges under pedestrian loading. The Technical Department for Transport, Roads and Bridges Engineering and Road Safety; 2006.
[24] BSI. NA to BS EN 1991-2:2003: UK National Annex to Eurocode 1: actions on structures – Part 2: traffice loads on bridges. London, UK: British Standards Institution; 2008.
[25] Živanović S, Pavić A, Ingólfsson Einar T. Modeling spatially unrestricted pedestrian

traffic on footbridges. J Struct Eng 2010;136:1296–308.
[26] Caprani CC, Ahmadi E. Formulation of human–structure interaction system models for vertical vibration. J Sound Vib 2016;377:346–67.
[27] Sudret B. Uncertainty propagation and sensitivity analysis in mechanical models–Contributions to structural reliability and stochastic spectral methods. Clermont-Ferrand, France: Habilitationa diriger des recherches, Université Blaise Pascal; 2007.
[28] Gautschi W. Orthogonal polynomials (in Matlab). J Comput Appl Math 2005;178:215–34.
[29] Wan HP, Ren WX, Todd MD. An efficient metamodeling approach for uncertainty quantification of complex systems with arbitrary parameter probability distributions. Int J Numer Meth Eng 2016;109:739–60.
[30] Sobol IM. Sensitivity estimates for nonlinear mathematical models. Math Modell Comput Exp 1993;1:407–14.
[31] Sudret B. Global sensitivity analysis using polynomial chaos expansions. Reliab Eng Syst Saf 2008;93:964–79.
[32] Wan HP, Ren WX. Parameter selection in finite-element-model updating by global sensitivity analysis using Gaussian process metamodel. J Struct Eng 2015;141:04014164.
[33] Smith M. ABAQUS/Standard User's Manual, Version 6.13-2. Providence, RI: Simulia; 2013.
[34] Wei X, Russell J, Živanović S, Mottram JT. The effects of hammer operator in manually operated impact hammer testing of lightweight structures. In: The 7th World Conference on Structural Control and Monitoring. Qingdao, China. 22 - 25 July, 2018.
[35] Živanović S. Probability-based estimation of vibration for pedestrian structures due to walking [PhD thesis] Sheffield, UK: University of Sheffield; 2006.
[36] Subbaraj K, Dokainish MA. A survey of direct time-integration methods in computational structural dynamics—II. Implicit methods. Comput Struct 1989;32:1387–401.
[37] Tsai CL, Daniel IM. Determination of in-plane and out-of-plane shear moduli of composite materials. Exp Mech 1990;30:295–9.
[38] Mottram JT. Shear modulus of standard pultruded fiber reinforced plastic material. J Compos Constr 2004;8:141–7.
[39] Gates P. Polymeric facades: advanced composites for retrofit [PhD thesis] University of Bath; 2013.
[40] Strongwell. FRP specifications-Section 06600: fiberglass reinforced polymer (FRP) products and fabrications. Bristol, USA; 2012.
[41] Nguyen T-T, Chan T-M, Mottram JT. Reliable in-plane shear modulus for pultruded-fibre-reinforced polymer sections. Proc Inst Civ Eng Struct Build 2017:1–12.
[42] Zureick A-H, Bennett RM, Ellingwood BR. Statistical characterization of fiber-reinforced polymer composite material properties for structural design. J Struct Eng 2006;132:1320–7.
[43] Strongwell. Design manual. Strongwell Corporation; 2010.
[44] Lekou DJ, Philippidis TP. Mechanical property variability in FRP laminates and its effect on failure prediction. Composites Part B 2008;39:1247–56.
[45] Zuniga MM, Kucherenko S, Shah N. Metamodelling with independent and dependent inputs. Comput Phys Commun 2013;184:1570–80.
[46] Navarro M, Witteveen J, Blom J. Polynomial Chaos Expansion for general multivariate distributions with correlated variables. arXiv preprint arXiv:1406.5483; 2014.
[47] Dey S, Mukhopadhyay T, Haddad Khodaparast H, Kerfriden P, Adhikari S. Rotational and ply-level uncertainty in response of composite shallow conical shells. Compos Struct 2015;131:594–605.
[48] Naskar S, Mukhopadhyay T, Sriramula S, Adhikari S. Stochastic natural frequency analysis of damaged thin-walled laminated composite beams with uncertainty in micromechanical properties. Compos Struct 2017;160:312–34.
[49] Kohavi R. A study of cross-validation and bootstrap for accuracy estimation and model selection. The 14th International Joint Conference on Artificial Intelligence. San Mateo, CA: Morgan Kaufmann; 1995. p. 1137–43.